Received: 9 December 2022 | Revised: 21 March 2023 | Accepted: 29 March 2023

DOI: 10.1111/cas.15804

Cancer Science WILEY

ORIGINAL ARTICLE

Plasma extracellular vesicle transcriptomics identifies CD160 for predicting immunochemotherapy efficacy in lung cancer

Jiatao Liao[1,2] | Hongyan Lai[1,2] | Chang Liu[1,2] | Xin Zhang[1,2] | Qiuxiang Ou[3] | Qiaojuan Li[1,2] | Yan Li[1,2] | Zhen Wang[1,2] | Cuicui Liu[3] | Xianghua Wu[1,2] | Huijie Wang[1,2] | Hui Yu[1,2] | Si Sun[1,2] | Xinmin Zhao[1,2] | Zhihuang Hu[1,2] | Yao Zhang[1,2] | Ying Lin[1,2] | Bo Yu[1,2] | Shenglin Huang[1,4] | Jialei Wang[1,2]

[1]Department of Thoracic Medical Oncology, Fudan University Shanghai Cancer Center, and Shanghai Key Laboratory of Medical Epigenetics, International Co-laboratory of Medical Epigenetics and Metabolism, Institutes of Biomedical Sciences, Shanghai Medical College, Fudan University, Shanghai, China

[2]Department of Oncology, Shanghai Medical College, Fudan University, Shanghai, China

[3]Geneseeq Research Institute, Nanjing Geneseeq Technology., Nanjing, Jiangsu, China

[4]Shanghai Key Laboratory of Radiation Oncology, Fudan University Shanghai Cancer Center, Shanghai, China

Correspondence
Jialei Wang, Department of Thoracic Medical Oncology, Fudan University Shanghai Cancer Center, 270 Dong An Road, Shanghai 200032, China.
Email: luwangjialei@126.com

Shenglin Huang, Shanghai Key Laboratory of Medical Epigenetics, International Co-laboratory of Medical Epigenetics and Metabolism, Institutes of Biomedical

Abstract

Better biomarkers are needed to improve the efficacy of immune checkpoint inhibitors in lung adenocarcinoma (LUAD) treatment. We investigated the plasma extracellular vesicle (EV)-derived long RNAs (exLRs) in unresectable/advanced LUAD to explore biomarkers for immunochemotherapy. Seventy-four LUAD patients without targetable mutations receiving first-line anti-programmed cell death 1 (PD-1) immunochemotherapy were enrolled. Their exLRs were profiled through plasma EV transcriptome sequencing. Biomarkers were analyzed against response rate and survival using pre- and post-treatment samples in the retrospective cohort ($n=36$) and prospective cohort ($n=38$). The results showed that LUAD patients demonstrated a distinct exLR profile from the healthy individuals ($n=56$), and T-cell activation-related pathways were enriched in responders. Among T-cell activation exLRs, CD160 exhibited a strong correlation with survival. In the retrospective cohort, the high baseline EV-derived CD160 level correlated with prolonged progression-free survival (PFS) ($P<0.001$) and overall survival (OS) ($P=0.005$), with an area under the curve (AUC) of 0.784 for differentiating responders from non-responders. In the prospective cohort, the CD160-high patients also showed prolonged PFS ($P=0.003$) and OS ($P=0.014$) and a promising AUC of 0.648. The predictive value of CD160 expression was validated by real-time quantitative PCR. We also identified the dynamics of EV-derived CD160 for monitoring therapeutic response. The elevated baseline CD160 reflected a

Abbreviations: AUC, area under the curve; BP, biological process; CI, confidence interval; circRNA, circular RNA; CR, complete response; CT, computed tomography; DEG, differentially expressed gene; dMMR, mismatch repair deficiency; EV, extracellular vesicles; exLR, extracellular vesicle-derived long RNA; FC, fold change; FDR, false discovery rate; GO, Gene Ontology; HR, hazard ratio; ICI, immune checkpoint inhibitor; IQR, interquartile range; KEGG, Kyoto Encyclopedia of Genes and Genomes; LDH, lactate dehydrogenase; lncRNA, long non-coding RNA; LUAD, lung adenocarcinoma; LUSC, lung squamous cell carcinoma; mRNA, messenger RNA; MSI, microsatellite instability; NK cell, natural killer cell; NLR, neutrophil-to-lymphocyte ratio; NSCLC, non-small cell lung cancer; ORR, objective response rate; OS, overall survival; PBMC, peripheral blood mononuclear cell; PD, progressive disease; PD-1, programmed cell death 1; PFS, progression-free survival; PLR, platelet-to-lymphocyte ratio; PR, partial response; RNA-seq, RNA sequencing; ROC, receiver operating characteristic; RT-qPCR, real-time quantitative PCR; SD, stable disease; TCGA, The Cancer Genome Atlas; TMB, tumor mutational burden; TPM, transcripts per kilobase million; tx, treatment.

Jiatao Liao, Hongyan Lai, and Chang Liu have contributed equally to this work and share first authorship.

Shanghai Municipal Health Commission, (Grant/Award Number: "2020CXJQ02") National Key Research and Development Project of China, (Grant/Award Number: "2021YFA1300500")

Sciences, Shanghai Medical College, Fudan University, 270 Dong An Road, Shanghai 200032, China.
Email: slhuang@fudan.edu.cn

Funding information
National Key Research and Development Project of China, Grant/Award Number: 2021YFA1300500; Shanghai Municipal Health Commission, Grant/Award Number: 2020CXJQ02

higher abundance of circulating NK cells and $CD8^+$-naïve T cells, suggesting more active host immunity. In addition, increased CD160 levels of tumors also correlated with a favorable prognosis in LUAD patients. Together, plasma EV transcriptome analysis revealed the role of the baseline CD160 level and early post-treatment CD160 dynamics for predicting the response to anti-PD-1 immunochemotherapy in LUAD patients.

KEYWORDS
extracellular vesicle, immunochemotherapy, lung adenocarcinoma, RNA sequencing, therapeutic biomarker

1 | INTRODUCTION

Lung cancer has been the leading cause of cancer-related mortality worldwide for many years. Lung adenocarcinoma (LUAD) represents the most common histological subtype, accounting for approximately 40% of lung cancers.[1,2] In recent years, immune checkpoint inhibitors (ICIs) targeting programmed cell death 1 (PD-1) and its ligand (PD-L1) have revolutionized the treatment of advanced non-small cell lung cancer (NSCLC) without targetable genetic mutations.[3] The PD-1 inhibitor has demonstrated great clinical efficacy in the first-line treatment of advanced LUAD when administered as monotherapy in patients with PD-L1 tumor proportion score ≥50% or in combination with platinum-based chemotherapy regardless of tumor PD-L1 expression.[4,5]

Biomarkers predicting immunotherapy response for lung cancer include the expression of PD-L1, tumor mutational burden (TMB), and microsatellite instability (MSI)/mismatch repair deficiency (dMMR).[4,6–8] However, NSCLC patients with low tumor PD-L1 expression or TMB may still benefit from PD-1 inhibitor plus chemotherapy.[5,9,10] MSI/dMMR is rare in lung cancer, with an incidence of less than 1%.[11] However, difficulties are often experienced in collecting multiple, sufficient lung tissue biopsies for use as tissue-based biomarkers. Due to the intra-tumoral spatial heterogeneity, single biopsy specimens may not be indicative of the whole tumor microenvironment (TME) and the systemic antitumor immune response.[12] Furthermore, the wide application of immunochemotherapy underscores the importance of new biomarker discovery, as studies have revealed that the predictive effectiveness of known ICI-related markers, such as PD-L1 and TMB, in LUAD weakens after the addition of chemotherapy to ICI.[5,13] Therefore, improved predictive biomarkers are needed to better stratify patients for their response to immunochemotherapy.

Extracellular vesicles (EVs), mainly including exosomes and microvesicles, are lipid-bilayered nanoparticles secreted from most cell types into the peripheral circulation.[14,15] Cargos carried by EVs contain different nucleic acids, proteins, and lipids, which may represent the parental cells of the EVs and mediate the functions of recipient cells.[16] Recently, EV-based liquid biopsy has gained increasing attention in the early diagnosis, progression monitoring, prognosis prediction, and therapy efficacy assessment of cancer.[17–19] Jin et al. reported that plasma EV-derived miRNAs could be used to distinguish LUAD from lung squamous cell carcinoma (LUSC) in the early diagnosis of NSCLC.[20] de Miguel-Perez et al. reported that EV PD-L1 dynamics could predict clinical response to ICIs in NSCLC patients.[21] EV-derived long RNAs (exLRs) mainly comprise messenger RNA (mRNA), circular RNA (circRNA), and long non-coding RNA (lncRNA).[22] Our previous studies have demonstrated exLRs are promising diagnostic and prognostic biomarkers of pancreatic ductal adenocarcinoma and breast cancer.[23–25] However, the potential role of exLRs in the ICI-based treatment of advanced NSCLC has yet to be investigated.

In this study, we profiled the plasma exLRs in locally advanced/metastatic LUAD patients without targetable oncogenic drivers and explored the potential of exLRs as predictive biomarkers to stratify patients for receiving first-line immunochemotherapy of the anti-PD-1 agent. Notably, we found that EV-derived CD160 may predict the immunochemotherapy efficacy in LUAD.

2 | MATERIALS AND METHODS

2.1 | Patients and samples

A total of 74 LUAD patients and 56 healthy participants were involved in this study at Fudan University Shanghai Cancer Center (Shanghai, China). The clinical stage was determined according to the eighth edition of the TNM staging system.[26] Patient inclusion criteria were: pathologically confirmed unresectable or metastatic LUAD that did not carry sensitizing EGFR/ALK/ROS1 mutations, treatment-naïve, and baseline Eastern Cooperative Oncology Group performance-status score of 0 or 1. PD-L1 expression was measured by Dako IHC 22C3 pharmDx assay. Specifically, the retrospective cohort included 36 patients consecutively enrolled between June 21, 2019 and July 31, 2020, and the prospective cohort consisted of 38 LUAD patients admitted between August 1, 2020 and July 31, 2021. All patients received PD-1 inhibitor (pembrolizumab or camrelizumab) intravenously in combination with pemetrexed and platinum (cisplatin or carboplatin) every 3 weeks for four to six cycles, followed by PD-1 inhibitor plus pemetrexed maintenance therapy every 3 weeks until disease progression or unacceptable toxicity.

Blood samples were collected from healthy donors ($n=56$), all LUAD patients before the first administration of immunochemotherapy (baseline, $n=74$), and the retrospective cohort during treatment (dynamic post-treatment, $n=46$). For dynamic post-treatment plasma specimens, 36 out of 46 samples were collected from the 36 patients after two cycles of immunochemotherapy, including five patients who developed PD after the first response evaluation. The remaining 10 samples were collected after four cycles of immunochemotherapy ($n=4$) and at the time of disease progression ($n=6$), respectively, except for patients who developed PD at the first response evaluation.

2.2 | Response evaluation

Response was evaluated according to the Response Evaluation Criteria in Solid Tumors version 1.1.[27] We defined progression-free survival (PFS) time as the date from the initiation of immunochemotherapy until either the occurrence of disease progression or death from any cause. Overall survival (OS) was defined as the date from the initiation of immunochemotherapy until the date of death from any cause. Patients who had not progressed or died at the time of the data cutoff date or who were lost to follow-up before progression or death at the time of their last contact were censored. The objective response rate (ORR) was defined as the proportion of patients with a complete response (CR) or partial response (PR) as the best overall response. Patients who achieved CR or PR as the best overall response during immunochemotherapy with PFS ≥6 months were defined as responders. Patients who achieved stable disease (SD) or progressive disease (PD) as the best overall response or patients with PFS <6 months were defined as non-responders.

2.3 | Plasma separation, extracellular vesicle purification, and extracellular vesicle-derived long RNA

Briefly, the EV and RNAs were isolated using an exoRNeasy Serum/Plasma Kit (Qiagen). Plasma separation, EV purification, and characterization (including transmission electron microscopy, size distribution measurement, and western blots), and exLR isolation are described in detail in the Supporting Information and carried out as previously described.[22,23]

2.4 | Extracellular vesicle-derived long RNA sequencing analysis

Extracellular vesicle-derived long RNAs isolated from plasma were treated with DNase I (NEB) to remove DNA. Strand-specific RNA-seq libraries were then prepared using the SMARTer Stranded Total RNA-seq kit (Clontech). Library quality was analyzed using a Qubit Fluorometer (Thermo Fisher Scientific) and Qsep100 (BiOptic); 2 × 150 bp paired-end sequencing was performed on an Illumina sequencing platform. The raw sequencing reads were filtered by FastQC (version 0.11.8) and aligned to the Gencode human genome (GRCh38) using the read aligner STAR (version 2.7.1a).[28] Gene expression levels were then quantified by featureCounts (version 1.6.3)[29] and transformed into transcripts per kilobase million (TPM). Annotation information of mRNA, lncRNA, and pseudogene genes were retrieved from the GENCODE database (Human, version 29). The circRNAs were discovered and quantified by the Assembling Splice Junctions Analysis software.[30]

2.5 | Data interpretation and statistics

RNA-seq read counts were converted to TPM values for scaling all comparable exLR genes across samples. Genes with overall low frequencies (expressed in less than 30% of all analyzed samples) were filtered out, and the remaining exLRs were used for subsequent analysis. Differences in exLR expression between responders and non-responders were evaluated using fold change (FC) and compared using the Mann–Whitney *U*-test. The Wilcoxon signed-rank test was conducted for comparisons of paired pre- and post-treatment samples from the same patient. ExLRs with FC >1.5 and $p<0.05$ were defined as statistically significant differentially expressed genes (DEGs). Gene Ontology (GO) biolocal process (BP) enrichment analysis and Kyoto Encyclopedia of Genes and Genomes (KEGG) pathway analysis were performed on the differentially expressed exLRs to determine the significantly dysregulated pathways. False discovery rate (FDR) was controlled using Benjamini–Hochberg adjustment.

Clinical characteristics of patients were summarized using median and interquartile range (IQR) for continuous variables and frequencies and percentages for categorical variables. For the clinical features of the retrospective and prospective groups, we performed the *t*-test on normally distributed continuous variables and the χ^2 or Fisher's exact test on categorical variables.

Patient survival data were estimated using the Kaplan–Meier method, and the statistical difference between groups was tested by log-rank test. The efficacy of EV-derived CD160 expression distinguishing responders from non-responders was evaluated using the receiver operating characteristic (ROC) curve. Prognostic factors associated with PFS and OS were identified by univariate and multivariate analysis using the Cox proportional hazards regression model. Variables with $p<0.05$ in the univariate analysis were included in the subsequent multivariate analysis. Proportional hazard models were used to estimate hazard ratios (HRs) and their 95% confidence intervals (CIs).

IBM SPSS Statistics (version 26) and R (version 4.0.2) tools were used in the statistical analysis. All *P*-values were analyzed using a two-sided test; values below 0.05 were considered statistically significant.

3 | RESULTS

3.1 | Patient overview

This study enrolled a total of 74 LUAD patients and 56 healthy individuals and (Table S1). Among the LUAD patients (Table S2), the median age was 63 years in the retrospective cohort ($n=36$) and 65 years in the prospective cohort ($n=38$). In both cohorts, most patients were male, previous or current smokers, in stage IV and common metastatic sites in the chest and bone. Eleven (19%) patients in the retrospective cohort had brain metastasis, while three (7.9%) patients in the prospective cohort had brain metastasis. The PD-L1 status is unknown for 36.1% and 50% of the retrospective and prospective cohorts, respectively. There were no significant differences between the two cohorts in terms of age, gender, stage, metastatic sites, or PD-1 inhibitors received (Table S2). At data cutoff (July 31, 2021), the median duration of follow-up was 11.75 months (IQR, 9.30–18.15 months) in the retrospective cohort and 7.73 months (IQR, 6.52–10.35 months) in the prospective cohort. The ORRs were 52.8% and 52.6% in the retrospective and prospective cohorts, respectively. A total of 15 (41.7%) patients in the retrospective cohort and 19 (50.0%) in the prospective cohort were classified as responders to immunochemotherapy.

3.2 | Extracellular vesicle-derived long RNA profiling in lung adenocarcinoma patients

To illustrate the exLRs profile of LUAD patients, we isolated RNA from baseline plasma EVs of 74 LUAD patients and 56 healthy donors and implemented exLR-seq for each plasma sample (Figure 1A). The isolated vesicles were rounded, cup-shaped, and double-membrane-bound, as observed by transmission electron microscopy (Figure 1B). Flow cytometry of the isolated vesicles revealed a heterogeneous population of spherical nanoparticles, with a mean diameter of 100.2 ± 37.1 nm (Figure 1C). Western blot analysis confirmed the enriched expression of EV markers CD63 and TSG101 in isolated vesicles but not in peripheral blood mononuclear cells (PBMCs). Meanwhile, the endoplasmic reticulum (ER) marker Calnexin, which is expected to be absent in EVs, was detected in PBMCs but not in isolated vesicles (Figure 1D).

Approximately 15,000 and 16,000 annotated exLR genes, including mRNAs, lncRNAs, pseudogenes, and circRNAs, were constantly detected in each sample of healthy donors and LUAD patients, respectively. Among the detected exLRs, most are mRNAs. The numbers of enriched mRNAs, pseudogenes, and circRNAs in LUAD patients were greater than those in healthy donors (Figure 1E). We identified 496 and 378 significantly upregulated and downregulated exLR genes, respectively, in LUAD patients compared with healthy donors (FDR < 0.05, FC > 2) (Figure 1F). KEGG pathway analysis revealed that differentially expressed exLRs were significantly enriched in cancer-associated pathways, such as transcriptional misregulation in cancer and NF-kappa B signaling pathway (Figure 1G).

3.3 | Baseline extracellular vesicle-derived CD160 level correlated with response to immunochemotherapy in lung adenocarcinoma patients

To identify exLR biomarks associated with treatment outcome, we first compared the baseline exLR expression profiles of responders and non-responders in the retrospective group. A total of 498 DEGs ($P<0.05$, FC > 1.5) were identified (Figure 2B). Gene ontology biological process (GO-BP) enrichment analysis indicated that the T-cell activation-related terms were significantly enriched in the DEGs (Figure 2C), suggesting the important role of T-cell activation in the responses to anti-PD-1 agent-based immunotherapy. We further explored the correlation between the baseline expression levels of those 17 annotated DEGs identified in the T-cell activation-related pathways (Figure 2C) and patients' PFS data. Patients were divided into high and low groups according to the median expression value of the corresponding gene. Among the T-cell-activating DEGs and non-T-cell-activating DEGs (genes identified as top DEGs except T-cell-activating genes), CD160 was most differentially expressed between responders and non-responders (Figures S1A and S2A), with the largest difference in median PFS in the retrospective cohort (Figure 2D; Figure S2B). The median PFS of baseline CD160-high patients was 19.80 months (95% CI, 9.00–30.60 months) versus 5.00 months (95% CI, 2.80–7.20 months) in the CD160-low patients (HR = 0.26, $P=0.001$, Figure 2E). In addition, in the prospective cohort, elevated CD160 levels also demonstrated a strong correlation with better PFS although not statistically significant ($P=0.06$, Figure S1B).

To further identify the optimal cutoff value of CD160 expression to classify patients' clinical benefit, we used the "maxstat" R package to divide the patients into baseline CD160 expression high and low subgroups by using the optimal cutoff value of 9.779. The median PFS was 19.82 months (95% CI, 13.10–26.54 months) in the CD160-high group versus 7.46 months (95% CI, 4.94–5.00 months) in the CD160-low group ($P<0.001$), with 5 (33.3%) versus 18 (85.7%) events of disease progression or death, respectively (Figure 3A). Prolonged OS was observed in the CD160-high group compared with the CD160-low group (median, not reached vs. 13.20 months [95% CI, 6.95–19.45 months]; $P=0.005$), with death occurring in 1 patient (6.7%) and 11 patients (52.4%), respectively (Figure 3B). To evaluate the prediction performance of baseline CD160 expression level, we performed ROC curve analysis and found the area under the curve (AUC) of 0.784 (95% CI, 0.619–0.949) with a sensitivity of 0.952 and a specificity of 0.600, implying its strong predictive ability (Figure 3C). Although the median survival time was not reached in the prospective cohort due to the relatively short follow-up, significantly prolonged PFS ($P=0.003$) and OS ($P=0.014$) were still observed in CD160-high patients by applying the cutoff value of 9.779 in the prospective cohort (Figure 3D,E). The AUC value of the ROC curve was 0.648 (95% CI, 0.467–0.829), with a sensitivity of 0.526 and a specificity of 0.789 (Figure 3F).

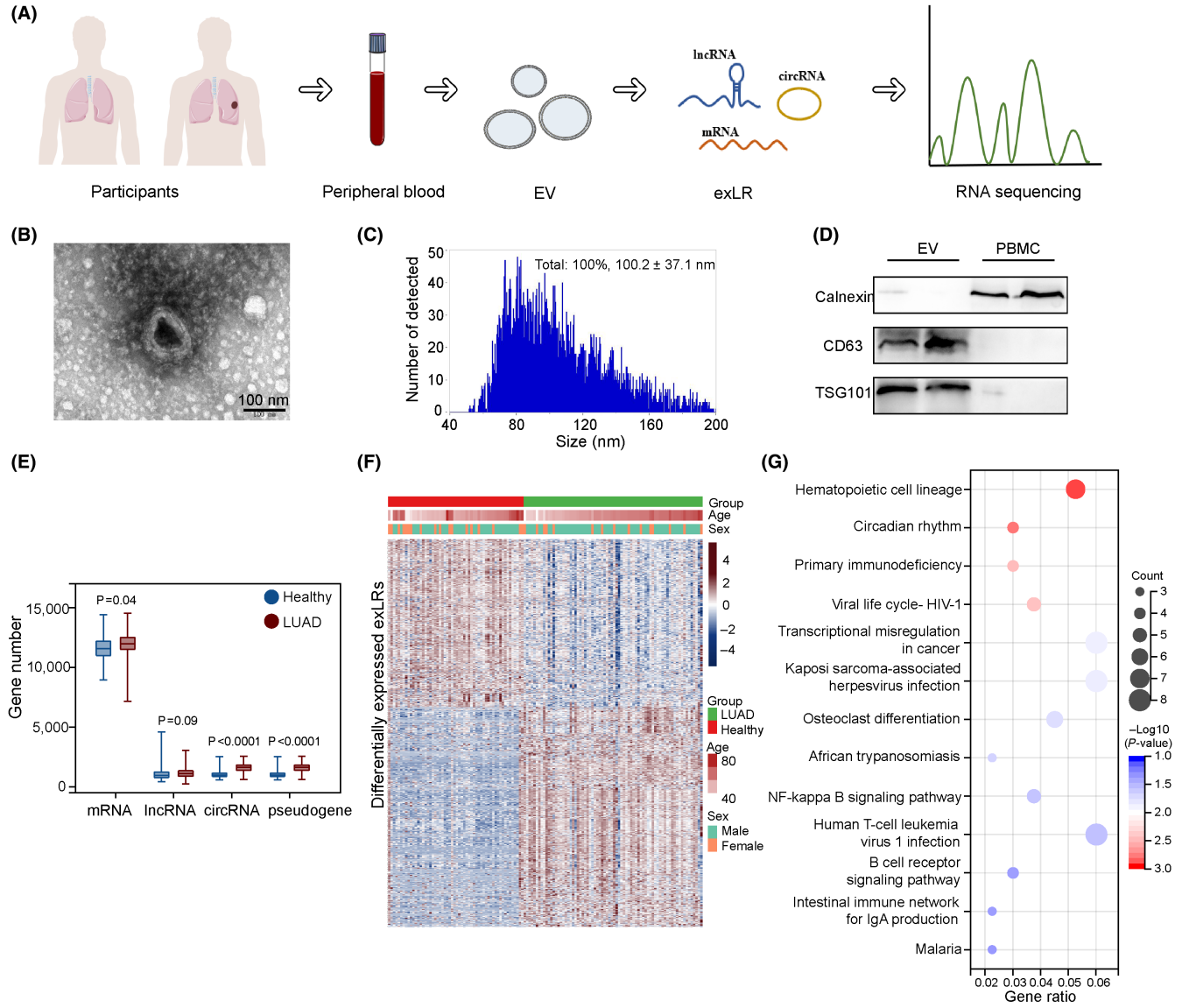

FIGURE 1 Extracellular vesicle-derived long RNA (exLR) profiling in lung adenocarcinoma (LUAD) patients and healthy individuals. (A) Workflow of extracellular vesicle (EV) extraction and exLR-seq. (B) Electron microscopy image of isolated EVs. (C) Size distribution measurements of isolated EVs. (D) Western blot analysis of exosome enrichment markers in the isolated EV and peripheral blood mononuclear cell (PBMC) factions from biological replicates of two patients. (E) Abundance of different exLRs per sample between LUAD patients and healthy subjects. (F) Heatmap showing 874 genes that are differentially expressed between LUAD patients and healthy donors. Differential expression was defined by fold change >2 and adjusted $p<0.05$. (G) KEGG enrichment analysis of differentially expressed exLRs between LUAD patients and healthy donors. Enriched pathways corresponding to other cancer types are not shown.

Next, we employed real-time quantitative PCR (RT-qPCR) analysis of RNA from the exLR sequencing library to validate the predictive value of baseline EV-derived CD160. Among the 41 measurable samples, the results revealed a high correlation with the exLR-seq data for EV-CD160 ($r=0.63$, $P<0.001$, Figure S3A), and an AUC of 0.656 (95% CI, 0.482–0.829) in predicting the clinical response (Figure S3B). Consistently, patients with high baseline CD160 level as determined by qPCR had significantly better survival than patients with low baseline CD160 level (Figure S3C,D, median PFS: not reached vs. 11.8 months, HR=0.37, $P=0.035$; median OS: not reached vs. 13.3 months, HR=0.22, $P=0.039$). Those findings strongly underscored the value of the baseline EV-derived CD160 in prediciting response.

We also checked if the EV-derived CD160 in LUSC ($n=30$) patients treated with anti-PD-1 immunochemotherapy could resemble the predictive function in LUAD. The expression of baseline CD160 was not significantly different between responders and non-responders (Figure S4A). The ROC curve of CD160 distinguishing responders from non-responders also showed unsatisfactory predictive capability (Figure S4B). We did not observe the survival difference (PFS and OS) between CD160-high and CD160-low groups (stratified by the median CD160 expression value) (Figure S4C,D). These data indicated that the expression level of baseline EV-derived CD160 for predicting the immunochemotherapy efficacy might be cancer type-specific.

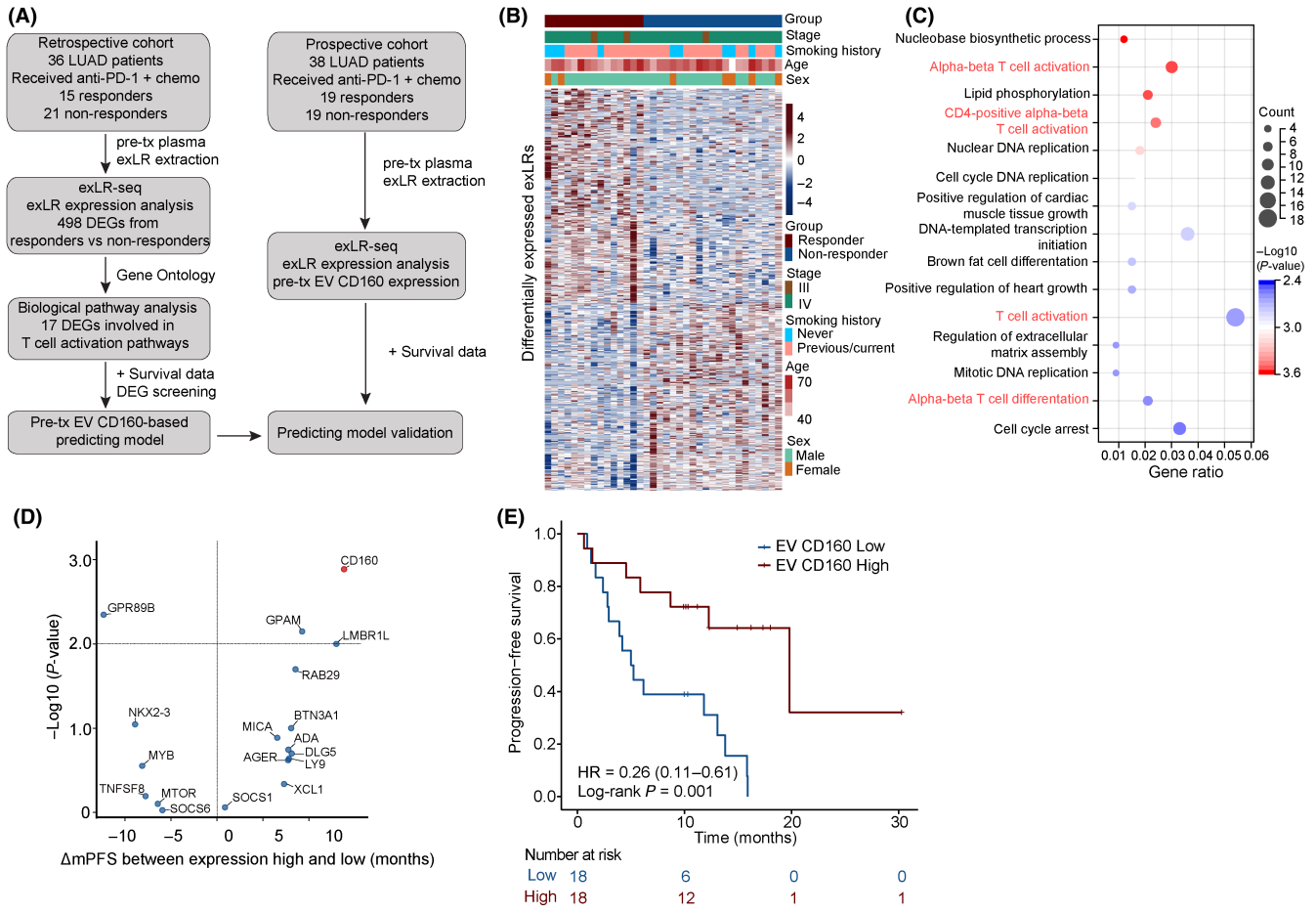

FIGURE 2 Identification of baseline extracellular vesicle (EV)-derived CD160 for stratifying patient treatment response. (A) Flowchart showing the selection and validation of CD160. (B) Heatmap showing the 498 differentially expressed EV-derived long RNAs (exLRs) between responders and non-responders in the retrospective cohort. (C) Top 15 significantly enriched GO-BP pathways analyzed from differentially expressed exLRs shown in (B). T-cell activation-related pathways are marked in red. (D) Summary of the log-rank *P*-values for progression-free survival (PFS) and the median PFS difference (ΔmPFS) associated with the identified T-cell activation-related genes. (E) PFS of the baseline EV-derived CD160 high and low lung adenocarcinoma (LUAD) patients divided by median CD160 expression level in the retrospective cohort.

3.4 | Monitoring the dynamic change of extracellular vesicle-derived CD160 for immunochemotherapy outcomes

The pre-treatment (pre-tx) and post-treatment (post-tx) blood samples from the LUAD patients of the retrospective cohort were used for paired exLR analysis. Notably, we found that the expression level of EV-derived CD160 in the responders significantly decreased from the baseline to early during treatment (the time point of the first imaging evaluation, approximately 4–6 weeks after the first administration of immunochemotherapy, $P = 0.002$, Figure 4A). However, such changes in CD160 expression were not observed in non-responders ($P = 0.56$, Figure 4A). Then, we divided all the retrospective patients into CD160-decrease and CD160-increase groups for analysis. Significantly prolonged both PFS ($P = 0.009$) and OS ($P = 0.007$) were observed in the CD160-decrease group compared with the CD160-increase group (Figure 4B,C). Hence, the change in blood EV-derived CD160 level early during the treatment may indicate the treatment outcomes for LUAD patients receiving anti-PD-1 immunochemotherapy.

To further evaluate the reflective role of EV-derived CD160 expression level changes for targeted lesion size during anti-PD-1 immunochemotherapy, we conducted longitudinal dynamic tracking of the CD160 expression and CT imaging in a representative patient who initially achieved PR but eventually experienced PD 13 months after treatment (Figure 4D). The CD160 expression level initially decreased when the patient showed PR at the first imaging evaluation point and kept decreasing with tumor shrinkage. The tumor began to progress after 13 months of treatment, and the CD160 expression level increased correspondingly. The entire course of tumor volume change by CT images and CD160 level change in this representative case is demonstrated in Figure 4D. The changes in EV-derived CD160 levels of this LUAD patient receiving anti-PD-1 immunochemotherapy are likely to reflect the clinical responses during treatment.

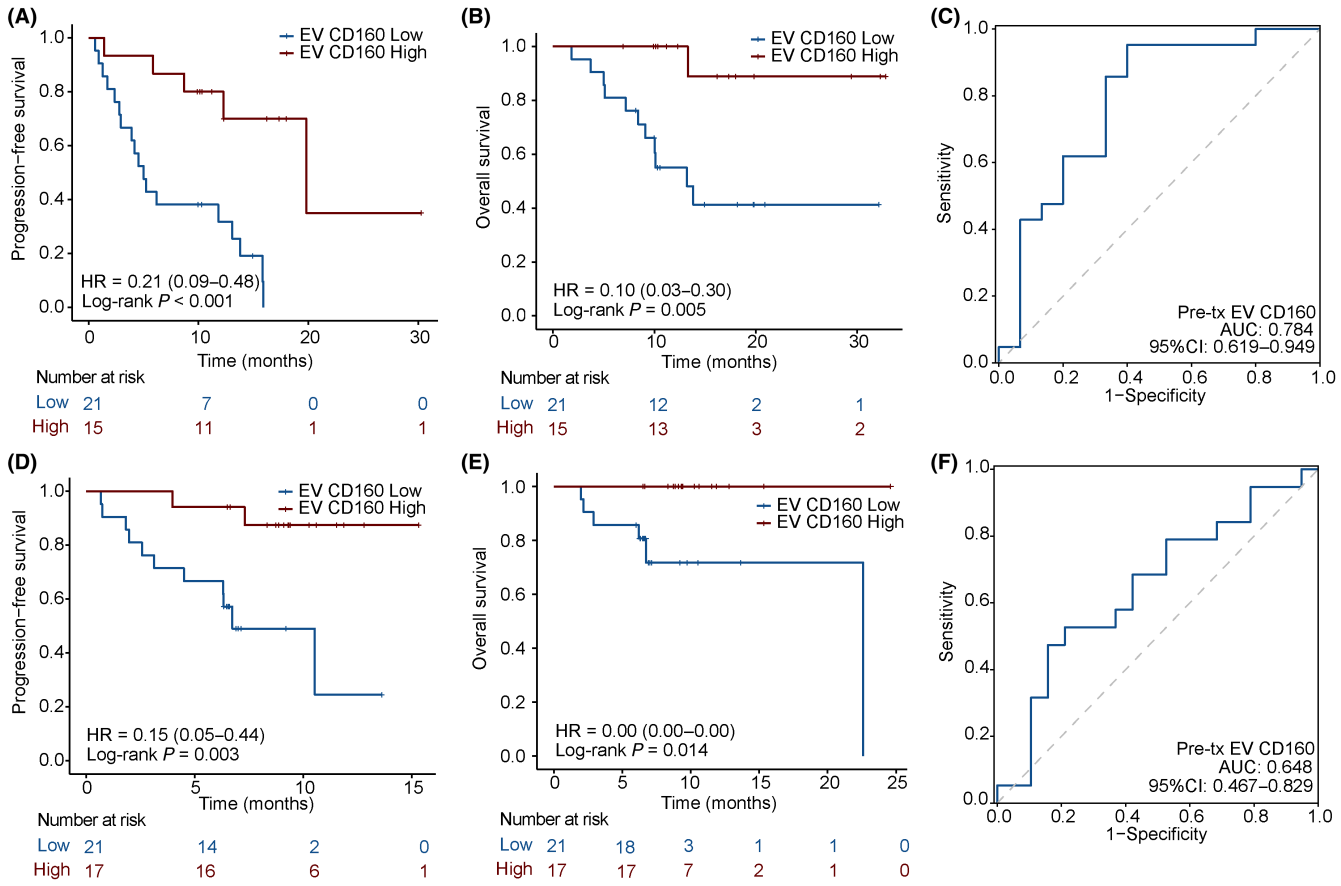

FIGURE 3 Performance validation of baseline extracellular vesicle (EV)-derived CD160 in response to immunochemotherapy. (A) Progression-free survival (PFS) and (B) overall survival (OS) of the baseline EV-derived CD160 high and low lung adenocarcinoma (LUAD) patients divided by the optimal cutoff of the baseline CD160 level in the retrospective cohort. (C) Receiver operating characteristic (ROC) curve of immunochemotherapy responders and non-responders based on the baseline EV-derived CD160 expression level in the retrospective cohort. (D) PFS and (E) OS of the baseline EV-derived CD160 high and low LUAD patients divided by the optimal cutoff of baseline CD160 level in the prospective cohort. (F) ROC curve of immunochemotherapy responders and non-responders based on the baseline EV-derived CD160 expression in the prospective cohort.

3.5 | Extracellular vesicle-derived CD160 interaction with other biomarkers in predicting response to immunochemotherapy

We further explored the interaction between EV-derived CD160 and other biomarkers using univariate and multivariate Cox regression analyses (Table 1). High NLR, high PLR, and high LDH are known immune-based biomarkers associated with inferior survival outcomes in NSCLC patients receiving immunotherapy.[31,32] The univariate analysis showed that the presence of bone metastases, high levels of NLR, and low baseline EV-derived CD160 expression were significantly associated with shorter PFS and OS, but the PD-1 inhibitor that patients received (pembrolizumab or camrelizumab) did not correlate with outcomes (Table 1). Aside from the presence of bone metastases and NLR, the multivariate analysis indicated baseline level of CD160 is also an independent prognostic factor for both PFS ($P=0.019$) and OS ($P=0.027$) (Table 1). We also assessed the predictive performance of baseline EV-derived CD160 in all LUAD patients with PD-L1 status available ($n=42$). No significant difference in baseline EV-derived CD160 expression was seen among different PD-L1 expression groups (Figure S5A). Despite the restricted cohort size, improved PFS and OS were still observed in the high CD160 groups across all PD-L1 categories (Figure S5B–G). In addition, both univariate and multivariate analyses showed a strong correlation between CD160 and PFS/OS, while the PD-L1 status failed to exhibit significant association with either outcome (Table S3). Together, those findings indicated the predictive role of EV-derived CD160 in LUAD, which is independent of the PD-L1 status (Figure S5).

When the CD160 expression level was used alone or in combination with other prognostic factors (high EV-derived CD160 level, low NLR level, and no bone metastasis), the ORRs (proportions of CR or PR as the best response) (Figure 5A) and duration of response of ≥6 months (Figure 5B) were all at high levels. Combining the baseline EV-derived CD160 expression level and NLR level from the hematological testing, we leveraged the predictive power of the resultant model (AUC=0.733) for all enrolled LUAD patients (Figure 5C). To establish a predicting model applicable in clinical use, we constructed a nomogram integrating the presence of bone metastasis,

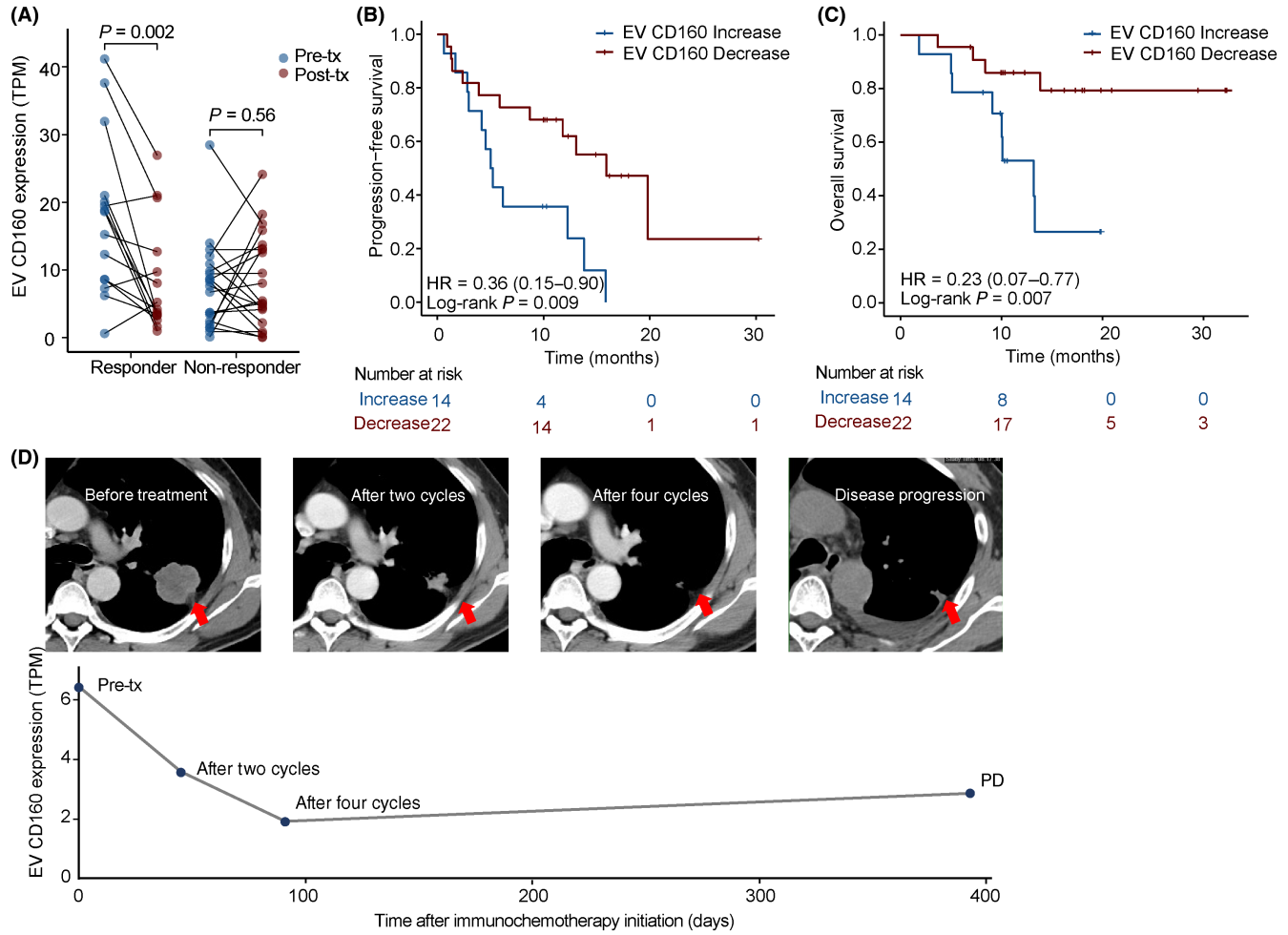

FIGURE 4 Dynamics of post-treatment extracellular vesicle (EV)-derived CD160 expression predicts response to chemoimmunotherapy in lung adenocarcinoma (LUAD). (A) The dynamic EV-derived CD160 changes early after treatment in responders and non-responders. (B) Progression-free survival (PFS) and (C) overall survival (OS) of the EV-derived CD160 level change in LUAD patients from the retrospective cohort. (D) The representative case showing the correlation between EV-derived CD160 level and tumor volume at the left lobe by CT imaging from initial response to drug resistance.

NLR level, and EV-derived CD160 level for 6-month PFS prediction by multivariate Cox regression in all enrolled LUAD patients (Figure 5D). We confirmed the discrimination degree, concordance, and clinical usefulness of the nomogram for its potential application in the patient's risk stratification (Figure S6). Collectively, our results suggested EV-derived CD160 as a potential prognostic factor that could leverage the predictive performance for clinical outcomes in patients with unresectable and metastatic LUAD.

3.6 | Potential mechanism of extracellular vesicle-derived CD160 regulation and lung adenocarcinoma patients' prognosis

We next attempted to understand the mechanism underlying the prognostic role of EV-derived CD160. An EV deconvolution approach, named EV-origin, was developed in our previous study to infer the tissue-cellular source contributions of EVs from the exLR-seq profiles.[33] Here, we utilized EV-origin to decipher the cellular origin heterogeneity of the circulating EVs between CD160-high and CD160-low expression cohorts. Compared to the CD160-low subset, the CD160-high subset showed the most significant enrichment of EVs originating from natural killer (NK) cells and $CD8^+$-naïve T cells (Figures 6A,B, and S7A), which implied a higher abundance of innate and adaptive immunity components in the CD160-high population. Furthermore, compared to non-responders, responders also tend to have a significantly higher EV-derived CD160 RNA levels from $CD8^+$-naïve T cells and NK cells (Figure S7B).

We further referred to the tissue-derived CD160 from the Cancer Genome Atlas (TCGA)-LUAD datasets to assess the concordance of CD160 expression between EVs and tissues in LUAD for predicting clinical outcomes. Overall, the CD160 expression was significantly lower in LUAD tissues than in noncancerous tissues (Figure 6C). Notably, the patients with a baseline high tissue CD160 level (above the third quartile) displayed a better prognosis than those with a baseline low tissue CD160 level (below the

TABLE 1 Univariate and multivariate Cox analyses for progression-free survival and overall survival in all lung adenocarcinoma patients.

		Progression-free survival		Overall survival	
Variable	**Categorization**	**Univariate HR (95% CI)**	**Multivariate HR (95% CI)**	**Univariate HR (95% CI)**	**Multivariate HR (95% CI)**
Age		1.000 (0.956–1.045), $P = 0.992$		1.001 (0.944–1.062), $P = 0.972$	
Gender	Male vs. Female	0.538 (0.263–1.101), $P = 0.090$		0.699 (0.242–2.021), $P = 0.509$	
Smoking history	Previous/current vs. Never	0.766 (0.382–1.537), $P = 0.453$		1.364 (0.439–4.236), $P = 0.591$	
Stage	III vs. IV	0.287 (0.039–2.105), $P = 0.220$		0.000 (0.000-Inf), $P = 0.998$	
Chest metastases	Yes vs. No	1.098 (0.561–2.147), $P = 0.785$		1.011 (0.384–2.661), $P = 0.983$	
Adrenal gland metastases	Yes vs. No	1.960 (0.875–4.389), $P = 0.102$		2.216 (0.718–6.833), $P = 0.166$	
Liver metastases	Yes vs. No	1.026 (0.391–2.691), $P = 0.959$		0.429 (0.057–3.248), $P = 0.413$	
Brain metastases	Yes vs. No	1.382 (0.627–3.048), $P = 0.422$		1.685 (0.593–4.787), $P = 0.328$	
Bone metastases	Yes vs. No	2.561 (1.309–5.013), $P = 0.006$	1.946 (0.981–3.861), $P = 0.057$	3.467 (1.275–9.426), $P = 0.015$	3.105 (1.102–8.743), $P = 0.032$
NLR		1.346 (1.184–1.529), $P < 0.001$	1.314 (1.148–1.503), $P < 0.001$	1.408 (1.216–1.630), $P < 0.001$	1.311 (1.120–1.534), $P < 0.001$
PLR		1.002 (0.998–1.005), $P = 0.312$		1.003 (0.999–1.008), $P = 0.105$	
LDH		1.001 (0.999–1.003), $P = 0.184$		1.001 (0.999–1.003), $P = 0.284$	
Programmed cell death 1 inhibitor	Camrelizumab vs. Pembrolizumab	0.892 (0.386–2.060), $P = 0.789$		1.756 (0.602–5.123), $P = 0.303$	
CD160		0.934 (0.894–0.976), $P = 0.002$	0.953 (0.915–0.992), $P = 0.019$	0.057 (0.008–0.431), $P = 0.006$	0.889 (0.801–0.987), $P = 0.027$

Abbreviations: HR, hazard ratio; LDH, lactate dehydrogenase; NLR, neutrophil-to-lymphocyte ratio; PLR, platelet-to-lymphocyte ratio.

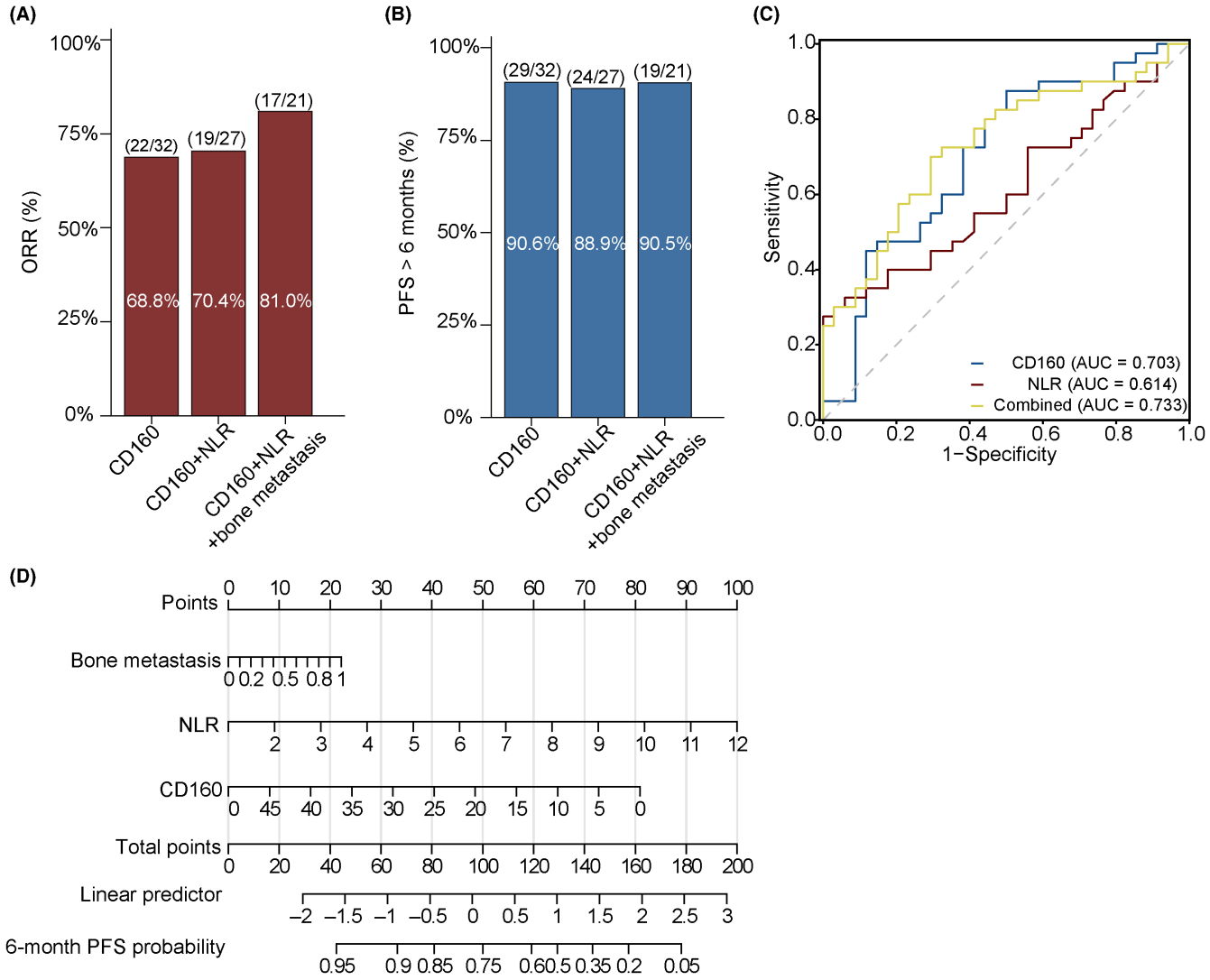

FIGURE 5 Interaction of EV-derived CD160 and other predicting indexes. (A) Objective response rate (ORR) in subgroups by different predicting indexes. Neutrophil-to-lymphocyte ratio (NLR) level was divided by optimal cutoff according to progression-free survival (PFS) (cutoff value 4.64). (B) Proportions of patients with PFS >6 months in subgroups by different predicting indexes. NLR level was divided by optimal cutoff according to PFS (cutoff value 4.64). (C) Receiver operating characteristic curves of baseline CD160 expression level, NLR, and the combined model in responders and non-responders. (D) A nomogram integrating the presence of bone metastasis, NLR level, and CD160 expression for predicting 6-month PFS for all enrolled lung adenocarcinoma patients.

first quartile) (Figure 6D), resembling the better response to immunochemotherapy observed in LUAD patients having a higher baseline EV-derived CD160 level. In addition, we analyzed the TCGA-LUSC datasets. Similar to the results of LUSC EVs, we observed no significant difference in overall survival between the low (below the first quartile) and high (above the third quartile) tissue CD160 level groups (Figure S8).

4 | DISCUSSION

To the best of our knowledge, this is the first study to implement a comprehensive analysis of plasma EV transcriptome in unresectable/advanced LUAD patients and identify predictive biomarkers for immunochemotherapy efficacy. From the transcriptome profiling of plasma EVs, we found that elevated baseline EV-derived CD160 is associated with better clinical outcomes in LUAD patients treated with anti-PD-1 immunochemotherapy, independently of other prognostic factors.

CD160, also known as BY55, is a member of the immunoglobulin superfamily mainly expressed on circulating NK cells and T cells.[34,35] There are different forms of CD160, including the glycosylphosphatidylinositol-anchored, transmembrane, and soluble forms.[36,37] The regulatory role of CD160 on NK cells and T cells is complex and can be either stimulatory or inhibitory depending on the cell type and CD160 form. CD160 could bind to classical and non-classical major histocompatibility complex-I molecules with low affinity to trigger NK cell cytotoxicity and cytokine production.[34,38] It may also co-stimulate with anti-CD3 antibodies to promote proliferation for activated $CD8^+$ T cells.[39] However, like PD-1, lymphocyte

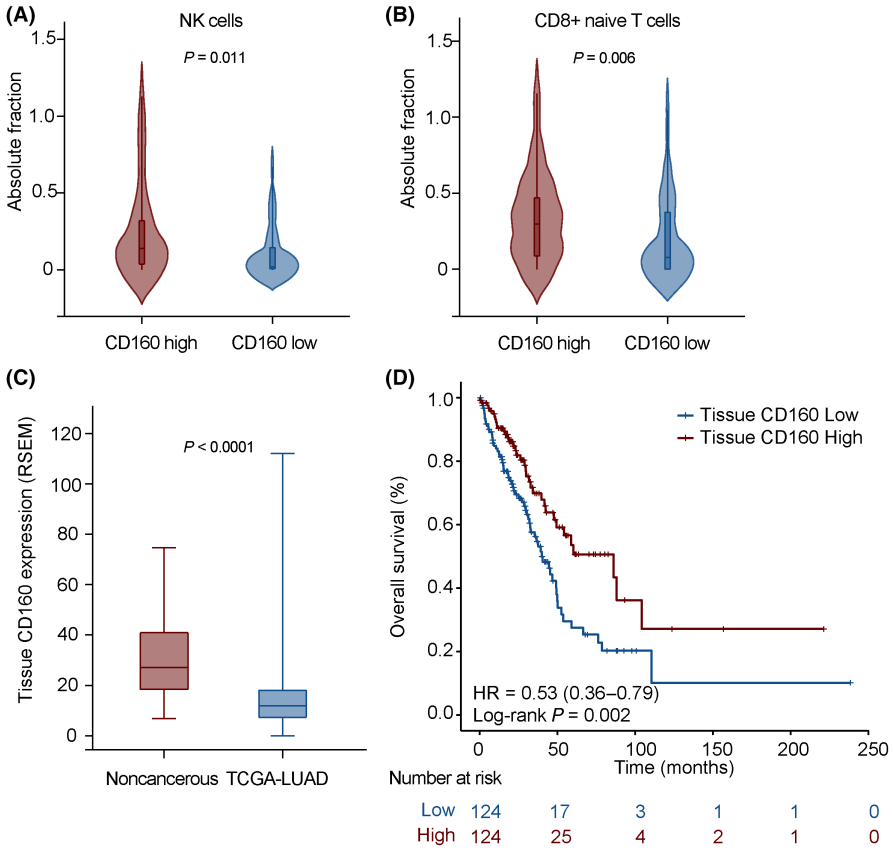

FIGURE 6 Tumor-derived CD160 level is also associated with favorable prognosis in lung adenocarcinoma (LUAD) patients. Violin plots showing that high baseline extracellular vesicle (EV) CD160 expression is significantly correlated with high abundance of (A) circulating natural killer (NK) cells and (B) circulating $CD8^+$-naïve T cells. (C) Boxplot showing that the CD160 expression in the cancerous tissue is significantly lower than in the adjacent normal tissue in the TCGA-LUAD dataset. (D) Overall survival (OS) of the TCGA-LUAD patients without targetable mutations in the CD160 high (top 25%) and CD160 low (bottom 25%) groups.

activation gene 3 (LAG-3), cytotoxic T-lymphocyte-associated antigen 4, T-cell immunoglobulin, and mucin domain-containing protein 3, CD160 is perceived as a co-inhibitory receptor on exhausted T cells and indicating the impaired T-cell effector function.[40,41] For instance, CD160-herpesvirus entry mediator is an immune-suppressive checkpoint.[34] The high-affinity interaction between them has been shown to inhibit $CD4^+$ T-cell activation and negatively regulate TCR-mediated $CD8^+$ T-cell signaling independently of PD-1 expression.[42,43] The CD160 antibody and PD-1 blockade combination could also enhance human immunodeficiency virus-specific T-cell responses.[37] However, another study showed that the higher baseline expression of CD160 on the $CD8^+$ cytotoxic T-cell subset correlates with a better response to antiretroviral therapy in patients with HIV infection.[44] In addition, it has been reported that $CD160^+CD8^+$ T cells displayed significantly higher cytotoxic function and proliferation than $CD160^-CD8^+$ T cells in chronic virus infection.[35] Thus, the above described discrepancies in the field warrant further investigations to comprehensively understand CD160 in the immune response.

The EV-origin analysis of pre-tx exLR revealed significantly more enriched fractions of EVs originating from NK cells and $CD8^+$-naïve T cells in CD160-high patients. We speculated that CD160 is an antigen-independent marker of general immune activation here, and the high EV-derived CD160 level could indicate an immune-active TME from the perspectives of NK cells and $CD8^+$-naïve T cells. Thus, the patients with higher pre-tx EV-derived CD160 levels benefited more from the PD-1 inhibition, as the PD-1/PD-L1 axis blockade would unleash the responses of NK cells and T cells in NSCLC.[45,46] For the CD160 decrease during the treatment in responders, we hypothesized that the expression change might reflect the reduction of inhibitory receptors, including CD160, upon the reinvigoration of exhausted T cells by PD-1 blockade. Additionally, a previous study has identified plasma EVs as a source of CD160 that could be taken up by T cells in patients with chronic lymphocytic leukemia.[47] In our study of LUAD, the high level of baseline EV-derived CD160 is likely to facilitate the therapeutic effect of PD-1 blockade, suggesting CD160 to be a potential target for immune intervention in LUAD patients. However, further investigation is needed to determine the origin of the EV-carried CD160.

We acknowledge several limitations of this study. First, this is a proof-of-principle study performed at a single center with a limited number of participants and a relatively short follow-up time in the prospective cohort. Thus, multicenter prospective studies with a larger sample size and a sufficiently long follow-up time would further verify our findings. Second, due to the multifaceted role of CD160, the underlying mechanism remains unclear. Our findings suggested that the high EV-derived CD160 level may reflect a more immune-active microenvironment, particularly attributed to NK cells and naïve T cells. However, it remains undetermined whether a general pro-immune activation mechanism is conferred by CD160 across different cancer modalities. Future research using larger sample sizes and broader cancer type portfolios with multi-omics analyses is warranted to provide more insight into the role of CD160.

AUTHOR CONTRIBUTIONS

Study concept and design: Shenglin Huang, Jialei Wang, and Jiatao Liao. *Patient management*: Xianghua Wu, Huijie Wang, Hui Yu, Si Sun, Xinmin Zhao, Zhihuang Hu, Yao Zhang, Ying Lin, and Bo Yu. *Data collection*: JL, Chang Liu, QL, XZ, YL, BY. *Data analyses*: HL, ZW, Cuicui Liu. *Manuscript writing*: Jiatao Liao, Hongyan Lai, and Chang Liu. *Manuscript revision*: Qiuxiang Ou, Jialei Wang, and Shenglin Huang. *Study supervision*: Jialei Wang and Shenglin Huang.

ACKNOWLEDGMENTS

The authors thank all the patients and healthy volunteers who participated in this study.

FUNDING INFORMATION

This study was sponsored by the Collaborative Innovation Cluster Program of Shanghai Municipal Health Commission (grant number: 2020CXJQ02) and the National Key Research and Development Project of China (grant number: 2021YFA1300500).

CONFLICT OF INTEREST STATEMENT

Cuicui Liu and Qiuxiang Ou are employees of Nanjing Geneseeq Technology, China. The remaining authors have no conflicts of interest to declare.

DATA AVAILABILITY STATEMENT

The datasets used and analyzed and materials used during the current study are available from the corresponding author upon reasonable request.

ETHICS STATEMENT

Approval of the research protocol by an Institutional Reviewer Board: The study was approved by the Institutional Review Board of the Fudan University Shanghai Cancer Center (Approval No. 2004216-20-2005) and was performed in compliance with the Declaration of Helsinki.

Informed consent: All informed consent was obtained from the subject(s) and/or guardian(s).

Registry and the registration no. of the study/trial: N/A.

Animal studies: N/A.

ORCID

Yan Li https://orcid.org/0000-0002-4655-9577
Ying Lin https://orcid.org/0000-0002-4321-0695
Jialei Wang https://orcid.org/0000-0001-9977-2219

REFERENCES

1. Schabath MB, Cote ML. Cancer progress and priorities: lung cancer. *Cancer Epidemiol Biomarkers Prev*. 2019;28:1563-1579.
2. Duma N, Santana-Davila R, Molina JR. Non-small cell lung cancer: epidemiology, screening, diagnosis, and treatment. *Mayo Clin Proc*. 2019;94:1623-1640.
3. Proto C, Ferrara R, Signorelli D, et al. Choosing wisely first line immunotherapy in non-small cell lung cancer (NSCLC): what to add and what to leave out. *Cancer Treat Rev*. 2019;75:39-51.
4. Mok TSK, Wu YL, Kudaba I, et al. Pembrolizumab versus chemotherapy for previously untreated, PD-L1-expressing, locally advanced or metastatic non-small-cell lung cancer (KEYNOTE-042): a randomised, open-label, controlled, phase 3 trial. *Lancet*. 2019;393:1819-1830.
5. Gadgeel S, Rodríguez-Abreu D, Speranza G, et al. Updated analysis from KEYNOTE-189: pembrolizumab or placebo plus pemetrexed and platinum for previously untreated metastatic nonsquamous non-small-cell lung cancer. *J Clin Oncol*. 2020;38:1505-1517.
6. Singal G, Miller PG, Agarwala V, et al. Association of patient characteristics and tumor genomics with clinical outcomes among patients with non-small cell lung cancer using a clinicogenomic database. *JAMA*. 2019;321:1391-1399.
7. Bodor JN, Boumber Y, Borghaei H. Biomarkers for immune checkpoint inhibition in non-small cell lung cancer (NSCLC). *Cancer*. 2020;126:260-270.
8. Rizvi NA, Hellmann MD, Snyder A, et al. Cancer immunology. Mutational landscape determines sensitivity to PD-1 blockade in non-small cell lung cancer. *Science*. 2015;348:124-128.
9. Langer C, Gadgeel S, Borghaei H, et al. OA04.05 KEYNOTE-021: TMB and outcomes for carboplatin and pemetrexed with or without pembrolizumab for nonsquamous NSCLC. *J Thorac Oncol*. 2019;14:S216.
10. Garassino M, Rodriguez-Abreu D, Gadgeel S, et al. OA04.06 evaluation of TMB in KEYNOTE-189: pembrolizumab plus chemotherapy vs placebo plus chemotherapy for nonsquamous NSCLC. *J Thorac Oncol*. 2019;14:S216-S217.
11. Duchemann B, Remon J, Naigeon M, et al. Current and future biomarkers for outcomes with immunotherapy in non-small cell lung cancer. *Transl Lung Cancer Res*. 2021;10:2937-2954.
12. Indini A, Rijavec E, Grossi F. Circulating biomarkers of response and toxicity of immunotherapy in advanced non-small cell lung cancer (NSCLC): a comprehensive review. *Cancer*. 2021;13:1794.
13. Garassino M, Rodriguez-Abreu D, Gadgeel S, et al. Evaluation of TMB in KEYNOTE-189: pembrolizumab plus chemotherapy vs placebo plus chemotherapy for nonsquamous NSCLC. *J Thorac Oncol*. 2019;14:S216-S217.
14. Colombo M, Raposo G, Théry C. Biogenesis, secretion, and intercellular interactions of exosomes and other extracellular vesicles. *Annu Rev Cell Dev Biol*. 2014;30:255-289.
15. van Niel G, D'Angelo G, Raposo G. Shedding light on the cell biology of extracellular vesicles. *Nat Rev Mol Cell Biol*. 2018;19:213-228.
16. Becker A, Thakur BK, Weiss JM, Kim HS, Peinado H, Lyden D. Extracellular vesicles in cancer: cell-to-cell mediators of metastasis. *Cancer Cell*. 2016;30:836-848.
17. Shi A, Kasumova GG, Michaud WA, et al. Plasma-derived extracellular vesicle analysis and deconvolution enable prediction and tracking of melanoma checkpoint blockade outcome. *Sci Adv*. 2020;6:eabb3461.
18. Zhou E, Li Y, Wu F, et al. Circulating extracellular vesicles are effective biomarkers for predicting response to cancer therapy. *EBioMedicine*. 2021;67:103365.
19. Chang L, Ni J, Zhu Y, et al. Liquid biopsy in ovarian cancer: recent advances in circulating extracellular vesicle detection for early diagnosis and monitoring progression. *Theranostics*. 2019;9:4130-4140.
20. Jin X, Chen Y, Chen H, et al. Evaluation of tumor-derived exosomal miRNA as potential diagnostic biomarkers for early-stage non-small cell lung cancer using next-generation sequencing. *Clin Cancer Res*. 2017;23:5311-5319.
21. de Miguel-Perez D, Russo A, Arrieta O, et al. Extracellular vesicle PD-L1 dynamics predict durable response to immune-checkpoint inhibitors and survival in patients with non-small cell lung cancer. *J Exp Clin Cancer Res*. 2022;41:186.
22. Li Y, Zhao J, Yu S, et al. Extracellular vesicles long RNA sequencing reveals abundant mRNA, circRNA, and lncRNA in human

blood as potential biomarkers for cancer diagnosis. *Clin Chem*. 2019;65:798-808.
23. Yu S, Li Y, Liao Z, et al. Plasma extracellular vesicle long RNA profiling identifies a diagnostic signature for the detection of pancreatic ductal adenocarcinoma. *Gut*. 2020;69:540-550.
24. Li Y, Li Y, Yu S, et al. Circulating EVs long RNA-based subtyping and deconvolution enable prediction of immunogenic signatures and clinical outcome for PDAC. *Mol Ther Nucleic Acids*. 2021;26:488-501.
25. Su Y, Li Y, Guo R, et al. Plasma extracellular vesicle long RNA profiles in the diagnosis and prediction of treatment response for breast cancer. *NPJ Breast Cancer*. 2021;7:154.
26. Amin MB, Greene FL, Edge SB, et al. The Eighth Edition AJCC Cancer Staging Manual: continuing to build a bridge from a population-based to a more "personalized" approach to cancer staging. *CA Cancer J Clin*. 2017;67:93-99.
27. Eisenhauer EA, Therasse P, Bogaerts J, et al. New response evaluation criteria in solid tumours: revised RECIST guideline (version 1.1). *Eur J Cancer*. 2009;45:228-247.
28. Dobin A, Davis CA, Schlesinger F, et al. STAR: ultrafast universal RNA-seq aligner. *Bioinformatics*. 2013;29:15-21.
29. Liao Y, Smyth GK, Shi W. featureCounts: an efficient general purpose program for assigning sequence reads to genomic features. *Bioinformatics*. 2014;30:923-930.
30. Zhao J, Li Q, Li Y, He X, Zheng Q, Huang S. ASJA: a program for assembling splice junctions analysis. *Comput Struct Biotechnol J*. 2019;17:1143-1150.
31. Van Wilpe S, Koornstra R, Den Brok M, et al. Lactate dehydrogenase: a marker of diminished antitumor immunity. *Onco Targets Ther*. 2020;9:1731942.
32. Mandaliya H, Jones M, Oldmeadow C, Nordman II. Prognostic biomarkers in stage IV non-small cell lung cancer (NSCLC): neutrophil to lymphocyte ratio (NLR), lymphocyte to monocyte ratio (LMR), platelet to lymphocyte ratio (PLR) and advanced lung cancer inflammation index (ALI). *Transl Lung Cancer Res*. 2019;8:886-894.
33. Li Y, He X, Li Q, et al. EV-origin: enumerating the tissue-cellular origin of circulating extracellular vesicles using exLR profile. *Comput Struct Biotechnol J*. 2020;18:2851-2859.
34. Piotrowska M, Spodzieja M, Kuncewicz K, Rodziewicz-Motowidło S, Orlikowska M. CD160 protein as a new therapeutic target in a battle against autoimmune, infectious and lifestyle diseases. Analysis of the structure, interactions and functions. *Eur J Med Chem*. 2021;224:113694.
35. Zhang L, Zhang A, Xu J, et al. CD160 plays a protective role during chronic infection by enhancing both functionalities and proliferative capacity of $CD8^+$ T cells. *Front Immunol*. 2020;11:2188.
36. Giustiniani J, Marie-Cardine A, Bensussan A. A soluble form of the MHC class I-specific CD160 receptor is released from human activated NK lymphocytes and inhibits cell-mediated cytotoxicity. *J Immunol*. 1950;2007(178):1293-1300.
37. El-Far M, Pellerin C, Pilote L, et al. CD160 isoforms and regulation of CD4 and CD8 T-cell responses. *J Transl Med*. 2014;12:217.
38. Le Bouteiller P, Barakonyi A, Giustiniani J, et al. Engagement of CD160 receptor by HLA-C is a triggering mechanism used by circulating natural killer (NK) cells to mediate cytotoxicity. *Proc Natl Acad Sci U S A*. 2002;99:16963-16968.
39. Agrawal S, Marquet J, Freeman GJ, et al. Cutting edge: MHC class I triggering by a novel cell surface ligand costimulates proliferation of activated human T cells. *J Immunol*. 1950;1999(162):1223-1226.
40. Wherry EJ, Kurachi M. Molecular and cellular insights into T cell exhaustion. *Nat Rev Immunol*. 2015;15:486-499.
41. Schietinger A, Philip M, Krisnawan VE, et al. Tumor-specific T cell dysfunction is a dynamic antigen-driven differentiation program initiated early during tumorigenesis. *Immunity*. 2016;45:389-401.
42. Cai G, Anumanthan A, Brown JA, Greenfield EA, Zhu B, Freeman GJ. CD160 inhibits activation of human $CD4^+$ T cells through interaction with herpesvirus entry mediator. *Nat Immunol*. 2008;9:176-185.
43. Viganò S, Banga R, Bellanger F, et al. CD160-associated CD8 T-cell functional impairment is independent of PD-1 expression. *PLoS Pathog*. 2014;10:e1004380.
44. Nikolova MH, Muhtarova MN, Taskov HB, et al. The CD160+ CD8high cytotoxic T cell subset correlates with response to HAART in HIV-1+ patients. *Cell Immunol*. 2005;237:96-105.
45. Trefny MP, Kaiser M, Stanczak MA, et al. PD-1(+) natural killer cells in human non-small cell lung cancer can be activated by PD-1/PD-L1 blockade. *Cancer Immunol Immunother*. 2020;69:1505-1517.
46. Ahn E, Araki K, Hashimoto M, et al. Role of PD-1 during effector CD8 T cell differentiation. *Proc Natl Acad Sci U S A*. 2018;115:4749-4754.
47. Bozorgmehr N, Okoye I, Oyegbami O, et al. Expanded antigen-experienced CD160(+)CD8(+)effector T cells exhibit impaired effector functions in chronic lymphocytic leukemia. *J Immunother Cancer*. 2021;9:e002189.

SUPPORTING INFORMATION

Additional supporting information can be found online in the Supporting Information section at the end of this article.

How to cite this article: Liao J, Lai H, Liu C, et al. Plasma extracellular vesicle transcriptomics identifies CD160 for predicting immunochemotherapy efficacy in lung cancer. *Cancer Sci*. 2023;114:2774-2786. doi:10.1111/cas.15804